Research Square

Preprints are preliminary reports that have not undergone peer review.
They should not be considered conclusive, used to inform clinical practice,
or referenced by the media as validated information.

Assessment of machining forces and surface integrity in face milling of CW50/PEEK under different thermal and cutting conditions

Carlos Gracioli Aita

carlos.aita@ifsc.edu.br

Federal Institute of Education Science and Technology of Santa Catarina: Instituto Federal de Educacao Ciencia e Tecnologia de Santa Catarina https://orcid.org/0000-0003-1522-9134

André João de Souza

UFRGS: Universidade Federal do Rio Grande do Sul

Émerson de Souza Passari

IFRS: Instituto Federal de Educacao Ciencia e Tecnologia do Rio Grande do Sul

Research Article

Keywords: CW50/PEEK face milling, cooled compressed air, heated compressed air, machining force, workpiece surface finish

Posted Date: November 11th, 2026

DOI: https://doi.org/10.21203/rs.3.rs-11503290/v1

License: This work is licensed under a Creative Commons Attribution 4.0 International License.
Read Full License

Assessment of machining forces and surface integrity in face milling of CW50/PEEK under different thermal and cutting conditions

Carlos A. G. Aita [1]*	carlosgracioliaita@gmail.com	0000-0003-1522-9134
André J. Souza [2]	ajsouza@ufrgs.br	0000-0001-5649-7333
Émerson S. Passari [2,3]	emerson.passari@gmail.com	0000-0002-8349-1348

[1] Federal Institute of Santa Catarina (IFSC), Xanxerê, SC, Brazil; *Corresponding author

[2] Federal University of Rio Grande do Sul (UFRGS), Porto Alegre, RS, Brazil

[3] Federal Institute of Rio Grande do Sul (IFRS), Ibirubá, RS, Brazil

Abstract: This study investigates how thermal and cutting conditions affect machining force (F_U) and workpiece surface finish during face milling of CW50/PEEK with a polycrystalline diamond tool. Four thermal conditions were evaluated across different cutting conditions using a 3-factor, 3-level Box-Behnken Design. Results showed that F_U was lowest under dry machining (DRY) due to matrix thermal softening and highest with cooled compressed air (CCA). Surface roughness analysis indicated R_a values below 1.0 µm, with most values ranging from 0.4 to 0.8 µm. DRY produced the lowest roughness values, whereas CCA resulted in the highest. Analysis of variance showed that axial depth of cut significantly affected F_U under DRY and heated compressed air (HCA) and even significantly influenced R_a under DRY and regular compressed air (RCA). Conversely, feed per tooth was significant for F_U under DRY and RCA, whereas the interaction between cutting speed and feed per tooth was significant for Ra only under DRY. Finally, scanning electron microscopy analysis revealed surface failures such as smearing, matrix debris, and fiber exposure, which varied with thermal condition. Overall, the results show that thermal condition plays a decisive role in face milling CW50/PEEK, influencing both machining force and workpiece surface finish.

Keywords: CW50/PEEK face milling, cooled compressed air, heated compressed air, machining force, workpiece surface finish.

1. INTRODUCTION

Carbon fiber-reinforced thermoplastics (CFRTP) have attracted increasing attention for high-performance structural applications because of their high specific strength, thermal stability, and excellent wear resistance. Among these materials, polyetheretherketone (PEEK)-based composites are notable for combining high mechanical strength, excellent thermal and chemical stability, and low density, making them attractive for applications in the aerospace, automotive, and biomedical industries [1–3]. Incorporating carbon fibers (CF) into PEEK significantly enhances its mechanical and tribological properties, further expanding its potential for components subjected to severe loading and temperature conditions [4, 5]. The performance of this CFRTP depends on factors such as matrix and reinforcement properties, as well as fiber architecture and orientation, which directly influence the material's anisotropic behavior [6–8]. Despite the advantages of CF/PEEK composites, machining operations are still often required to achieve dimensional accuracy, tight tolerances, and high surface quality in the final components [9]. However, the heterogeneous and anisotropic nature of these materials makes machining particularly challenging and can lead to defects such as fiber pull-out, delamination, and matrix degradation [10]. In this context, the integrity of the machined surface is a critical factor in assessing the machinability of CFRTP [6].

During the machining of carbon fiber-reinforced polymers (CFRP), the low thermal conductivity of the polymer matrix promotes heat buildup in the cutting zone, potentially raising the temperature above the glass transition temperature (T_g) of the polymer and altering the material removal mechanisms [11]. In addition, the high hardness and abrasiveness of the carbon fiber reinforcement intensify friction at the tool–workpiece interface, contributing to higher cutting temperatures and accelerating tool wear [12]. These factors make thermal control of the machining process essential for improving the machining performance of CF/PEEK composites. Traditionally, CFRP machining is performed under dry machining (DRY) conditions because conventional cutting fluids can adversely affect the polymer matrix properties, particularly through moisture absorption [13, 14]. However, dry machining can lead to high tool wear rates and poor surface quality. As an alternative, several cooling and lubrication strategies have been investigated to improve machining performance. Among them, minimum quantity lubrication (MQL) delivers a small amount of lubricant mixed with compressed air as an aerosol [15], although the generation of oil mist may pose health risks to machine operators [16]. Another approach is cryogenic machining, which uses fluids such as liquid nitrogen (LN_2) or dense mist generating by sublimating

solid carbon dioxide (SCO_2) to reduce the temperature in the cutting zone. Previous studies have shown that cryogenic cooling can reduce tool wear, surface roughness, and cutting temperature during CFRP machining [17–19]. However, this technique may increase machining forces because the material's stiffness rises at low temperatures, and it also entails additional costs and specific safety requirements [11, 20].

As a simpler and more sustainable alternative, compressed-air strategies have been increasingly used in machining processes. Compressed air offers low cost, wide availability in industrial environments, and lower environmental impact compared with conventional liquid cutting fluids [21, 22]. Although gases have lower heat-removal capacity than liquids, high-velocity air jets can promote heat dissipation while facilitating chip breakage and evacuation from the cutting zone [23]. Therefore, recent studies have investigated the use of compressed air under diverse thermal conditions in CFRP machining. Klein et al. [22] observed that cooled compressed air (CCA) improves the CF/epoxy surface finish and reduces machining-induced damage compared with dry machining (DRY) in end milling. Nor-Khairusshima et al. [24] also reported improved tool life and less delamination during CCA-assisted milling of a CFRTP hybrid laminate. Jia et al. [25] indicated that temperatures from −10 °C to 25 °C are favorable for end milling of multidirectional CF/epoxy. Pasquali et al. [26] investigated the effects of CCA and HCA on the surface finish of CF30/PEEK during face milling, reporting the lowest and highest surface roughness under CCA and HCA, respectively. Aita et al. [27] demonstrated that using CCA at −60 °C during face milling of PEEK reinforced with woven carbon fiber fabric (CW) significantly reduced machining forces and surface roughness compared with DRY.

The effects of temperature are particularly relevant for PEEK because of its thermomechanical behavior. The secondary transition temperature ($T_\beta \approx -60$ °C) is linked to changes in toughness and damping capacity [28]. Experimental studies have shown that reducing the temperature to values near this transition may promote a ductile-to-brittle transition, thereby influencing chip formation mechanisms during machining [29]. Conversely, controlled heating approaches have also been investigated, demonstrating the potential to reduce machining forces through matrix softening at temperatures just below the glass transition temperature ($T_g \approx 140$ °C) [30, 31].

Despite the growing number of studies on thermal control strategies for machining carbon fiber-reinforced polymers (CFRP), the literature remains limited in systematic investigations of how compressed air temperature affects milling carbon fiber-reinforced thermoplastics (CFRTP),

particularly reinforced with CW [27]. Furthermore, only three studies have specifically addressed the milling of CW/PEEK composites: one focused on machining force prediction [32] , another on specific cutting energy modeling [33] and a third compared cooled compressed air (CCA) and dry (DRY) conditions during milling using a WC tool [27] . Therefore, no systematic investigation has yet evaluated how different compressed air temperatures affect the milling behavior of this material. To address this gap, the present study investigates the face milling of the CW50/PEEK composite (polyetheretherketone reinforced with 50% woven carbon fiber fabric) using a polycrystalline diamond (PCD) tool under four thermal conditions: dry machining (DRY), regular compressed air at 24 °C (RCA), cooled compressed air at −40 °C (CCA), and heated compressed air at 60 °C (HCA). The objective is to understand how these thermal conditions affect the tool's cutting action, machining forces, and workpiece surface finish, thereby contributing to the development of more efficient and sustainable face milling strategies for CFRTP.

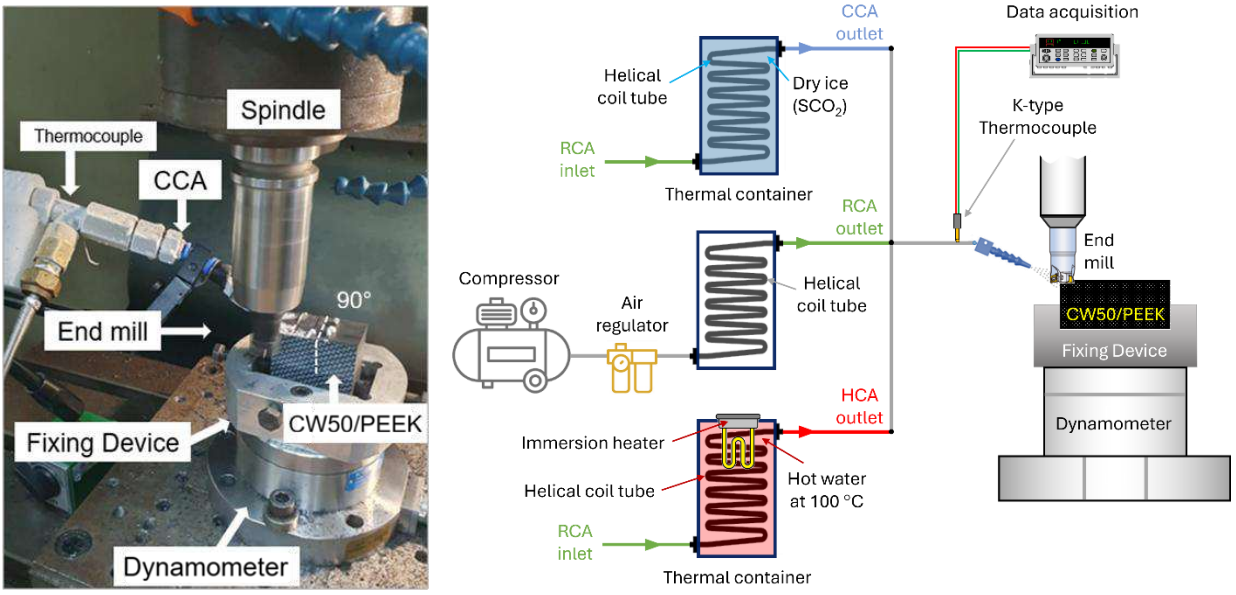
2. MATERIALS AND METHODS

The material used in this study was Ensinger® TECATEC PEEK MT CW50. This composite is manufactured by compression molding a VICTREX® PEEK matrix reinforced with 50% woven carbon fiber fabric (5HS HT 3K) in a 0°/90° fiber orientation. The CW50/PEEK has a density of 1.52 g/cm³, a tensile strength of 713 MPa, a glass transition temperature of 143 °C, a melting temperature of 343 °C, and a continuous service temperature of 260 °C (long-term) and 300 °C (short-term) [34].

Face milling was performed on a Romi® Discovery 308 machining center (maximum power of 5.5 kW and maximum spindle speed of 4000 rpm). Sandvik R390-11T304E-P4-NL CD10 carbide inserts with polycrystalline diamond (PCD) cutting tips were used, with a tool-nose radius (r_ε) of 0.4 mm, a cutting-edge radius (r_β) of 4.5 µm, and a wiper facet of 2.2 mm. A pair of inserts was mounted on a Sandvik CoroMill® 390 end-mill cutter with a nominal diameter of 20 mm. To ensure high machining accuracy, the tool was clamped hydraulically using a Sandvik CoroChuck® 930, providing less than 2.0 µm of runout.

A 61.0 × 40.6 × 26.6 mm workpiece was machined in multiple runs with a radial depth of cut (a_e) of 11.5 mm to optimize the use of this high-cost material and prevent damage to the samples. Across 60 face milling runs, the total cutting length was approximately 1890 mm, corresponding

to about 9 min of machining time without replacing the cutting edges. The tool paths were performed perpendicularly (90°) to the stacking direction of the woven carbon fiber fabric. Using a DinoLite® AM-413ZT digital microscope, no significant tool wear or microchipping was observed throughout the experiments. **Fig. 1a** shows the experimental setup for the cooled compressed air (CCA) condition, in which an 8 mm Y-shaped tube splitter directs the compressed air at a 45° inclination and a 20 mm distance from the cutting zone. The compressed air supply system (**Fig. 1b**) was designed to provide three air conditions: cooled compressed air (CCA), heated compressed air (HCA), and regular compressed air (RCA).



(a) (b)

Fig. 1. Experimental setup: (a) Image of CCA condition; (b) Scheme for compressed air devices.

Under the CCA condition, compressed air at 400 kPa flowed through a 30 m-long helical aluminum coil with an inner diameter of 8 mm, placed inside a thermally insulated container filled with dry ice (solid CO_2) at −78 °C. This setup enabled heat exchange, lowering the air temperature before it reached the cutting zone. Air temperature was monitored with a K-type thermocouple (−100 to 1000 °C) and recorded by an Agilent 34970A data acquisition system. The system was initially charged with 7.0 kg of dry ice, with an average refill rate of approximately 1.0 kg/h. Machining trials under the CCA condition began one minute after the air temperature stabilized at −40 ± 1 °C. Because of moisture in the compressed air and the low temperature of the solid CO_2,

inline air filters were installed to prevent coil blockage. Under the HCA condition, the same coil was immersed in a thermally insulated container filled with boiling water (100 °C), heated by two immersion heaters, thereby increasing the air temperature before it reached the cutting zone. The machining trials began one minute after the air temperature stabilized at 60 ± 3 °C. For the RCA condition, compressed air supplied directly from the pneumatic line flowed through the same coil at 24 ± 1 °C, without heating or cooling, ensuring flow rate characteristics and pressure losses comparable to those of the CCA and HCA conditions.

A Box-Behnken Design (BBD) was used to evaluate the effects of cutting speed (v_c), feed per tooth (f_z), and axial depth of cut (a_p), each at three levels, on surface roughness and machining force. Factor levels were selected based on a literature review and constraints imposed by spindle speed, the workpiece clamping system, and workpiece dimensions. Experiments were conducted in batches to minimize day-to-day variability. 15 machining runs were performed under each thermal condition: DRY, RCA (24 °C), CCA (–40 °C), and HCA (60 °C). The experimental design was generated using Minitab® 22 (trial version), and the corresponding cutting parameter combinations are presented in **Tab. 1**.

Tab. 1. Cutting parameter combinations for 15 machining runs.

Runs	v_c (m/min)	f_z (µm/tooth)	a_p (mm)	Runs	v_c (m/min)	f_z (µm /tooth)	a_p (mm)
1	150	75	1.1	9	200	50	0.5
2*	200	75	0.8	10	200	100	1.1
3	150	75	0.5	11	250	50	0.8
4	250	75	1.1	12	200	100	0.5
5	150	50	0.8	13	150	100	0.8
6	250	75	0.5	14*	200	75	0.8
7	200	50	1.1	15	250	100	0.8
8*	200	75	0.8				

*Central points defined by BBD

The orthogonal components of the machining force (F_x, F_y, and F_z) were measured in each experiment using a Kistler® 9272 stationary piezoelectric dynamometer. The signals were

conditioned by a Kistler® 5070A charge amplifier and acquired with a Measurement Computing PCIM-DAS 1602/16 data acquisition board on a dedicated computer. The data were processed in LabVIEW™ 9.0 at a sampling rate of 1 kHz. The resultant machining force (F_U) was calculated from 2000 samples collected, excluding the tool entry and exit regions during cutting.

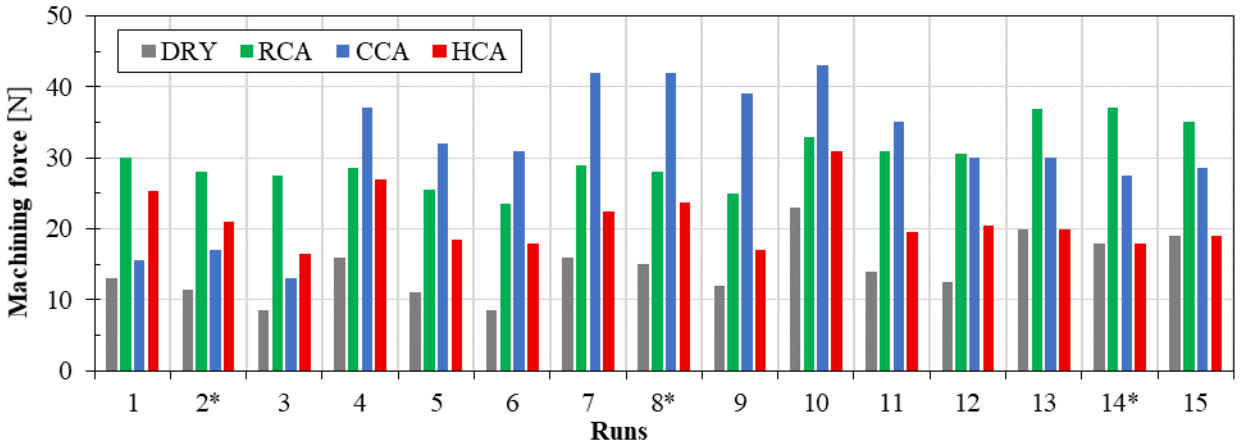
Two-dimensional surface roughness was evaluated using a Mitutoyo SJ-201P portable roughness tester (0.01 µm resolution). Three measurements were taken from each machined sample, with a sampling length of 0.8 mm and an evaluation length of 4.0 mm, following ISO 21920-3 recommendations for the range $0.1 < R_a < 2.0$ µm and non-periodic profiles [35]. R_a values were statistically analyzed in Minitab® 22 (trial version) with analysis of variance (ANOVA) and optimized using the Box-Behnken Design.

For complementary analysis of the optimized surfaces (three-dimensional surface profile and S_a and S_z parameters), a Taylor Hobson® Talysurf CCI-Lite white-light interferometer was used. Data processing was performed using MountainsMap® software integrated with the equipment. Finally, the surface topography of the machined samples was analyzed by scanning electron microscopy (SEM) on a Zeiss® EVO MA10 microscope.

3. RESULTS AND DISCUSSION

3.1. Machining Force

Fig. 2 presents the average machining force (F_U) values generated during face milling. Overall, machining forces were low across all thermal conditions. **Tab. 2** summarizes the mean F_U values for the 15 runs evaluated under each thermal condition, along with their standard deviations, and the maximum and minimum mean values recorded for each condition. Among the thermal conditions investigated, the lowest F_U was observed under the DRY condition, with an average machining force of approximately 14.5 N across all runs, followed by HCA (21.2 N), RCA (29.9 N), and CCA (30.8 N).



Runs	1	2*	3	4	5	6	7	8*	9	10	11	12	13	14*	15
v_c (m/min)	150	200	150	250	150	250	200	200	200	200	250	200	150	200	250
f_z (µm/tooth)	75	75	75	75	50	75	50	75	50	100	50	100	100	75	100
a_p (mm)	1.1	0.8	0.5	1.1	0.8	0.5	1.1	0.8	0.5	1.1	0.8	0.5	0.8	0.8	0.8

Fig. 2. Plot of collected F_U values under different cutting and thermal conditions.

The heat generated by tool-workpiece friction and material deformation tends to accumulate within the cutting zone under the DRY condition. Because PEEK has inherently low thermal conductivity, this heat is not readily dissipated, increasing the local cutting temperature and consequently causing the polymer matrix to soften. As a result, the material exhibits reduced shear strength, leading to lower machining forces [36].

Tab. 2. Values of F_U under each thermal condition.

Thermal condition	Mean F_U [N]	Std deviation [N]	Max F_U [N]	Min F_U [N]	Difference [N]
DRY	14.5	4.2	23.0	8.5	14.5
RCA	29.9	4.1	37.0	23.5	13.5
CCA	30.8	9.6	43.0	13.0	30.0
HCA	21.2	4.1	31.0	16.5	14.5

The increase in machining forces observed under the CCA and RCA conditions can be attributed to enhanced heat removal from the cutting zone, which reduces thermal softening of the

polymer matrix during machining. In CF/PEEK composites, the mechanical properties of the matrix are highly temperature-dependent, and a lower temperature tends to increase its stiffness and shear strength during the cutting operation. [36]. Furthermore, the similarity in F_U values under the RCA and CCA conditions may be attributed to the predominance of fiber fracture mechanisms during machining of the CW50/PEEK composite. Material removal in these composites involves carbon fiber fracture, matrix deformation, and fiber-matrix interfacial debonding, while the overall mechanical resistance is governed primarily by the reinforcing fibers [37]. Under the CCA condition, more intense cooling may further stiffen the polymer matrix and reduce its ductility, hindering plastic deformation around the carbon fibers and increasing resistance to material removal [17–19]. Similarly, under the RCA condition, although compressed air is supplied at room temperature, the airflow promotes convective heat removal from the cutting zone, limiting the temperature rise in the material caused by friction at the cutting edge [38]. This effect likely reduces thermal softening of the polymer matrix, making the material slightly stiffer and increasing its shear strength, resulting in higher F_U than those observed under the DRY condition [36].

When the reference runs (2*, 8*, and 14*) were evaluated, similar percentage variations were observed under the DRY (14.0%), RCA (14.0%), and HCA (14.5%) conditions, whereas a substantially higher variation was noted under the CCA condition (25.8%). This suggests that the CCA condition was more susceptible to uncontrolled input factors.

Tab. 3 presents the ANOVA results for F_U across the thermal conditions at the 90% confidence level. Under the DRY condition, the quadratic model achieved a satisfactory coefficient of determination (R^2). The linear effects of a_p and f_z, along with the quadratic effect of f_z, were statistically significant. These results indicate that the input factors strongly influenced F_U under this thermal condition. For the RCA condition, the R^2 value was close to the minimum recommended threshold, indicating a marginal fit of the quadratic model [39]. Under this thermal condition, only the linear effect of f_z was statistically significant, highlighting a change in process behavior compared to the DRY condition. For the CCA condition, the model did not achieve a satisfactory R^2, indicating that the factors did not significantly influence F_U. This behavior suggests that thermal effects associated with intensified cooling were predominant, reducing the sensitivity of the process with variations in cutting conditions. Regarding the HCA condition, only the linear effect of a_p was significant, indicating behavior distinct from the other thermal conditions. In addition, the model achieved a satisfactory R^2. This result suggests that heating the cutting zone

promoted greater heat penetration into the material, increasing the volume of material effectively affected by the process and making a_p a dominant variable affecting F_U. Conversely, f_z becomes less relevant, as thermal softening of the matrix reduces its influence on F_U [31].

Tab. 3. Reduced ANOVA for F_U under each thermal condition.

Thermal condition	R^2 [%]	Factors	Contribution [%]	P-Valor
DRY	89	f_z	23	0.02
		a_p	36	0.01
		$f_z \times f_z$	13	0.07
RCA	71	f_z	33	0.06
CCA	60	-	-	-
HCA	88	a_p	62	<0.01

As shown in **Tab. 3**, the coefficient of determination was insufficient for the CCA condition and low for RCA, indicating that the model has limited ability to describe machining-force variability based solely on controllable input factors. This behavior reinforces the predominant influence of thermal conditions, which modify the cutting mechanisms of the CW50/PEEK and reduce process sensitivity to cutting conditions. Therefore, under the CCA and RCA conditions, thermal effects tend to overcome the influence of input factors and govern the machining-force response. Under the DRY condition, the absence of external thermal assistance resulted in three statistically significant factors, demonstrating that, without thermally induced effects, F_U is predominantly governed by cutting conditions. Under the HCA condition, heated compressed air increased the temperature, promoting a certain degree of softening of the thermoplastic matrix [38]. This behavior can be attributed to its direct relationship with the subsurface layers of the material affected by heating in the cutting zone, indicating that the thermal softening promoted by HCA makes the axial depth of cut the dominant variable affecting the F_U response.

The standardized effects plots for F_U, with a significance level of $\alpha < 0.10$, are presented in **Fig. 3** as a complementary analysis to the ANOVA results. Points beyond the reference line indicate statistically significant effects.

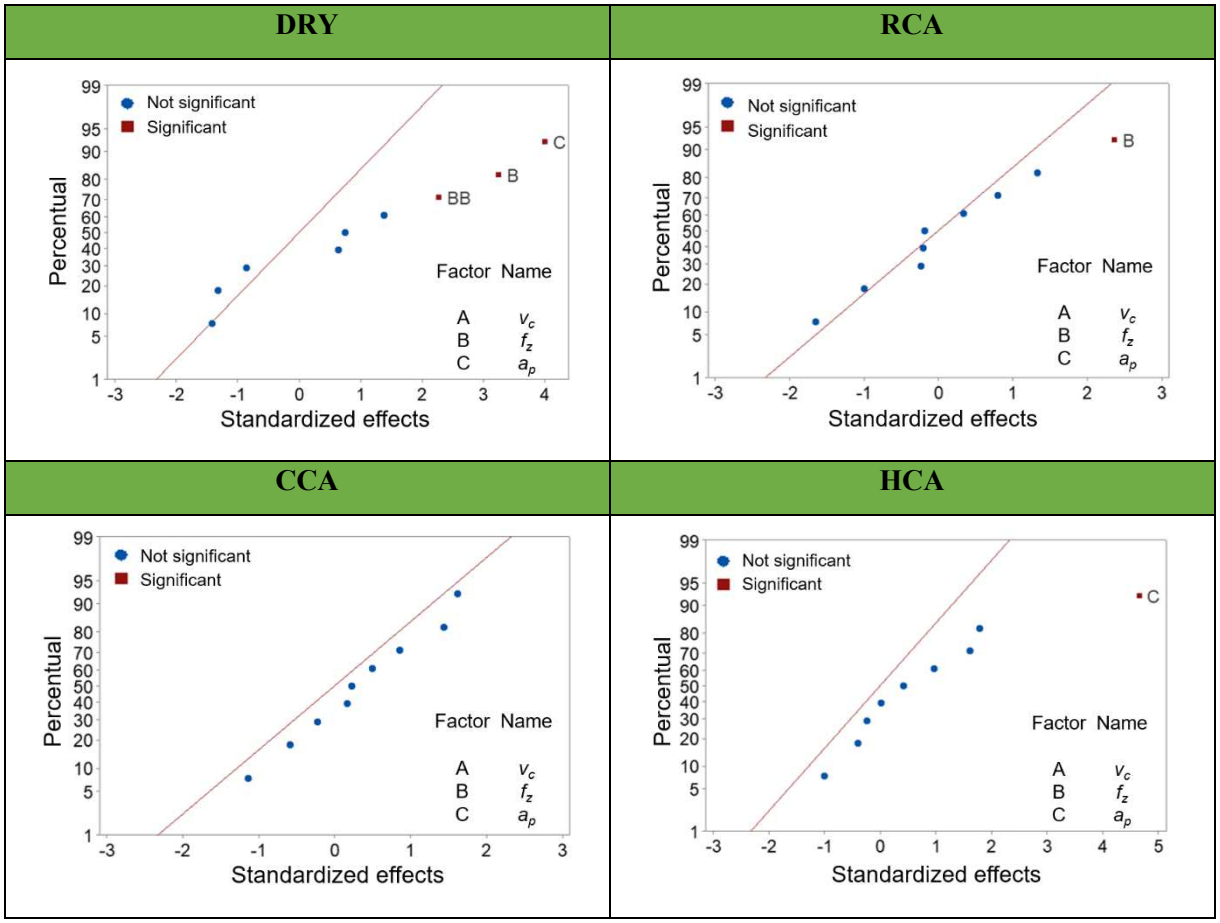


Fig. 3. Plot of standardized effects for F_U under different thermal conditions.

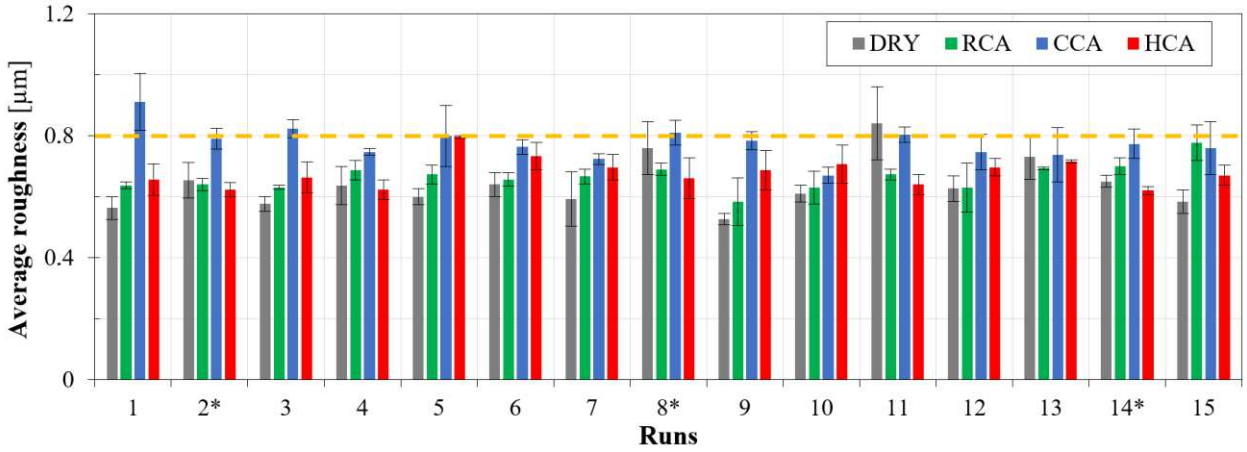
Significant effects were observed for the factors f_z (B), f_z x f_z (BB), and a_p (C) under the DRY condition, confirming that input factors have a more pronounced influence on F_U without thermally assisted conditions. For the RCA condition, only the linear effect of f_z (B) was statistically significant, indicating that the other parameters had less influence when compressed air at 24 °C was applied. This result may be associated with the slight cooling effect promoted by the airflow. For the CCA condition, no significant factors were identified, suggesting that air cooling was the dominant mechanism governing the F_U response and reducing process sensitivity to cutting conditions. This behavior may be related to changes in the mechanical properties of the matrix (PEEK) under low-temperature conditions, such as increased stiffness and embrittlement. Under the HCA condition, only the linear effect of a_p (C) was statistically significant, indicating that this parameter remains relevant even under heating conditions, with F_U tending to rise as a_p increases.

Higher cutting forces tend to increase the mechanical stresses at the fiber-matrix interface, promoting damage mechanisms and consequently increasing surface roughness. Studies on machining fiber-reinforced polymers have shown that machining force is strongly correlated with the roughness parameters obtained after milling, since higher forces can intensify fiber fracture and localized matrix deformation [40]. Therefore, because the thermal conditions investigated in this study influence the force levels during face milling, they are also expected to affect the development of the surface texture of the CW50/PEEK. Accordingly, the following subsection analyzes the surface roughness behavior of the machined surfaces.

3.2. Surface Integrity

Fig. 4 shows the arithmetic mean values of the average roughness (R_a) measured under the different thermal conditions. For all machined surfaces, R_a values remained below 1.0 μm, regardless of the thermal condition, corresponding to a surface roughness grade N7. Additionally, most runs resulted in values between 0.4 and 0.8 μm (grade N6). Not all runs achieved this grade, possibly due to variations in cutting conditions across the thermal conditions. The orange dashed line represents the upper limit of the N6 roughness grade. The lowest R_a values for each thermal condition were obtained for the following samples: DRY_{09} (0.53 μm), RCA_{09} (0.58 μm), HCA_{14} (0.62 μm), and CCA_{10} (0.67 μm).

A promising result was observed under the HCA condition, with all samples exhibited $R_a < 0.8$ μm, suggesting that heating during machining may have reduced their surface roughness. This behavior is linked to thermal softening of the matrix, which reduces brittle fracture and promotes more stable material removal. Kim et al.[31] reported similar findings on burr formation during heat-assisted CF/PA6 drilling with an industrial robot, attributing it to localized heating during the process. Likewise, Yan et al. [38] observed reductions of 13.56% in the arithmetic mean height of a surface (S_a) and 10.26% in the root mean square height of a surface (S_q) during grinding CF/PEEK at high temperature (170 to 180 °C) using a hot-air blowpipe, compared with grinding at room temperature (25 °C).



Runs	1	2*	3	4	5	6	7	8*	9	10	11	12	13	14*	15
v_c (m/min)	150	200	150	250	150	250	200	200	200	200	250	200	150	200	250
f_z (µm/tooth)	75	75	75	75	50	75	50	75	50	100	50	100	100	75	100
a_p (mm)	1.1	0.8	0.5	1.1	0.8	0.5	1.1	0.8	0.5	1.1	0.8	0.5	0.8	0.8	0.8

Fig. 4. Plot of collected R_a values under different cutting and thermal conditions

Conversely, the CCA condition exhibited a distinct behavior, with the mean surface roughness values being generally higher than those obtained under the other thermal conditions. In 10 of the 15 measured samples, R_a values remained above 0.8 µm, suggesting that cooling adversely affected the machined surface quality. This behavior may be associated with matrix stiffening at low temperatures, which favors mechanisms such as fiber fracture and fiber–matrix interfacial debonding, resulting in greater surface irregularity [37]. In addition, material shearing during cutting, followed by cooling in the high-temperature region, may alter the crystallinity of the thermoplastic matrix and directly affect the properties of CW50/PEEK [41]. However, the mechanisms through which temperature affects these properties are not yet fully understood.

Conversely, the CCA condition revealed a distinct behavior, with mean R_a values generally higher than under the other thermal conditions. In 10 of the 15 measured samples, R_a values remained above 0.8 µm, indicating that cooling degraded the machined surface quality. This behavior may be linked to matrix stiffening at low temperatures, which favors mechanisms such as fiber fracture and fiber-matrix interfacial debonding, leading to greater surface irregularity [37]. In addition, material shearing during cutting, followed by cooling in the high-temperature region, may have altered the crystallinity of the thermoplastic matrix and directly affected the properties

of CW50/PEEK [41]. However, the mechanisms by which temperature influences these properties are not yet fully understood.

Tab. 4 presents the overall mean R_a values for the samples analyzed from different cutting and thermal conditions, along with their respective standard deviations and the maximum and minimum R_a values observed for each condition. Thus, the lowest value was obtained under the DRY condition (0.64 µm), followed by RCA (0.67 µm), HCA (0.69 µm), and CCA (0.77 µm). The standard deviations among the thermal conditions were similar and relatively low, indicating good process repeatability.

Tab. 4. Values of R_a under each thermal condition

Thermal condition	Mean R_a [µm]	Std deviation [µm]	Max R_a [µm]	Min R_a [µm]	Difference [µm]	ISO Grade Number
DRY	0.64	0.05	0.84	0.53	0.31	N6-N7
RCA	0.67	0.03	0.78	0.58	0.11	N6
CCA	0.77	0.04	0.91	0.67	0.14	N6-N7
HCA	0.69	0.03	0.80	0.62	0.11	N6

Although the DRY condition produced the lowest overall R_a value across all samples, it also showed the greatest variability, indicating that changes in cutting conditions significantly affect the response variable. This behavior underscores the importance of parameter optimization to improve surface quality and process efficiency, thereby reducing costs and resource consumption [41]. Conversely, the CCA condition performed worse, confirming the previous discussion that intensive cooling does not further improve surface quality. The RCA and HCA conditions, in turn, generally performed satisfactorily. Notably, under all thermal conditions, the mean R_a values remained within the limits of roughness grade N6; however, grade N5 (0.2–0.4 µm) could not be reached. Therefore, from a practical standpoint, the DRY and RCA conditions are the most feasible and cost-effective alternatives for finish face milling of the CW50/PEEK, provided that appropriate cutting conditions are used.

Tab. 5 presents the analysis of variance (ANOVA) results for the effects of the controllable input factors on R_a, considering a 90% confidence level under the DRY, RCA, CCA, and HCA

conditions. For the CCA and HCA conditions, the complete quadratic model did not exhibit a satisfactory coefficient of determination (R^2 < 70%), indicating that variations in the cutting conditions did not significantly affect surface roughness; in these cases, the influence of the thermal conditions was greater than that of the cutting conditions. Conversely, under the RCA and DRY conditions, the statistical models exhibited satisfactory R^2 values (83% and 86%, respectively), and the quadratic effect of the axial depth of cut (a_p x a_p) was statistically significant for *Ra* under both thermal conditions. Under the DRY condition, the interaction between cutting speed and feed per tooth (v_c x f_z), was also significant, possibly due to the influence of heat generation and the well-established importance of feed rate on surface quality.

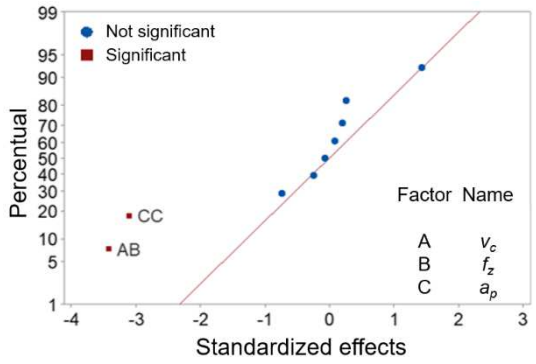
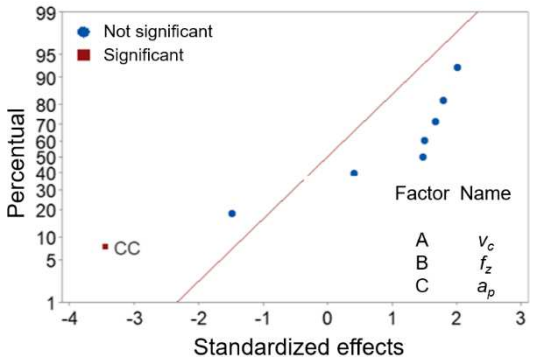
Tab. 5. Reduced ANOVA for R_a under each thermal condition

Thermal condition	R^2 [%]	Factors	Contribution [%]	P-Valor
DRY	83	a_p x a_p	33	0,03
		v_c x f_z	40	0,02
RCA	86	a_p x a_p	34	0,02
CCA	66	-	-	-
HCA	65	-	-	-

It is worth noting that, under both conditions, no linear effect was statistically significant, including f_z, a parameter commonly associated with the roughness of machined surfaces. This behavior may be attributed to the properties of the PCD insert, which features a sharp cutting edge, high hardness, and high thermal conductivity [42]. These characteristics can, in general, minimize the individual effects of input factors and thermal conditions on the quality of the machined surface. For example, Rodriguez et al. [43] found that the geometric parameters of the drill used for drilling CF/epoxy composites had a greater impact on surface integrity than the cooling conditions (SCO_2 and SCO_2 + MQL). Thus, under the conditions investigated, the results indicate that the characteristics of the PCD tool play a predominant role in determining surface roughness, often outweighing the effects of cutting conditions and thermal conditions.

Fig. 5 presents the standardized effects plots for the *Ra* response under the different thermal conditions, considering a significance level of α < 0.1. Under the DRY condition, statistically

significant effects were observed for the quadratic effect of a_p x a_p (factor CC) and the interaction between v_c x f_z (fator AB). Under the RCA condition, only the quadratic effect of a_p x a_p (factor CC) was statistically significant. Under both thermal conditions (DRY and RCA), these effects were located to the left of the reference line, indicating that increasing these factors is associated with a reduction in surface roughness. Under the CCA and HCA conditions, none of the analyzed factors (v_c, f_z e a_p), including linear and quadratic effects and their interactions, exhibited statistical significance. This suggests that the thermal effects, whether induced by cooling (CCA) or heating (HCA), override the direct influence of the input factors by modifying the conditions within the cutting zone. However, these modifications may be either beneficial or detrimental. The absence of statistically significant variables does not necessarily imply poorer performance but rather indicates the predominance of thermal effects. Indeed, the CCA condition exhibited the highest R_a values, whereas HCA maintained satisfactory performance despite the absence of significant effects from the cutting conditions. This further supports the notion that thermal control can be a determining factor in process response, regardless of variations in conventional cutting conditions.

DRY	RCA
	
CCA	**HCA**

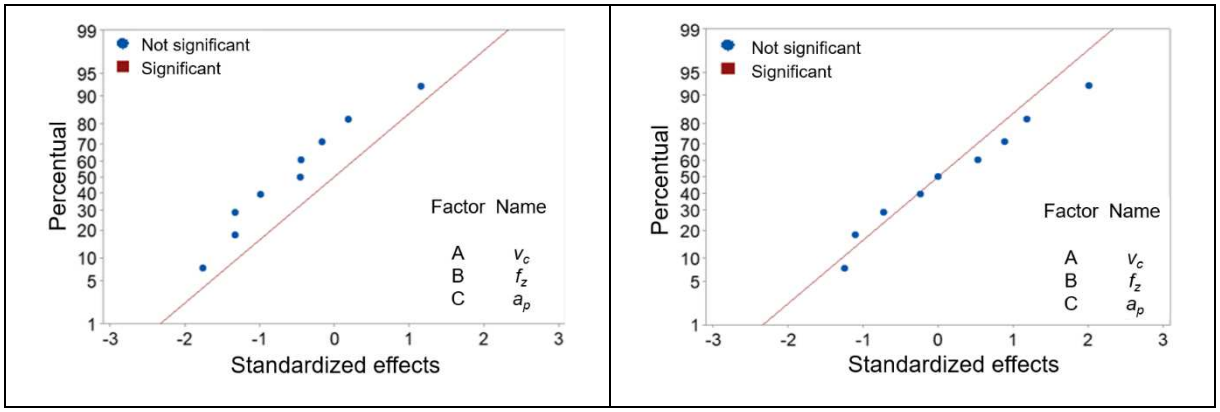
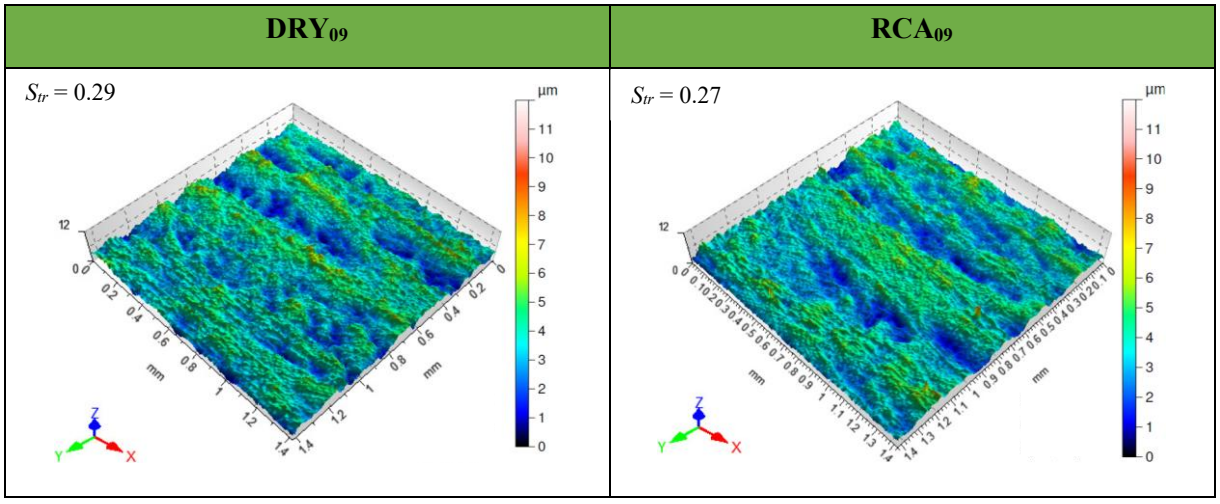


Fig. 5. Plot of standardized effects for R_a under different thermal conditions

Fig. 6 presents the 3D morphology of four samples selected based on their lowest R_a values under each thermal condition (DRY$_{09}$, RCA$_{09}$, CCA$_{10}$, and HCA$_{14}$). The 3D roughness parameters obtained for the different samples were similar (S_a = 0.48–0.53 µm; S_q = 0.60–0.67 µm; S_z = 6.40–6.80 µm), indicating highly similar surface profiles. These results further support the notion that the properties of the PCD tool prevailed over the effects of the thermal conditions. Individual height parameters may be insufficient for a comprehensive characterization of 3D surface texture; spatial, hybrid, or functional parameters can provide additional information for a more complete surface characterization [44]. Accordingly, the *Str* (texture aspect ratio) parameter was analyzed to quantify the spatial uniformity of the surface texture. A surface is considered anisotropic (*Str* < 0.5) when the texture exhibits a preferential direction, such as the feed marks left by the cutting tool [45]. Thus, the CCA$_{10}$ and HCA$_{14}$ samples exhibited the most uniform surface textures.



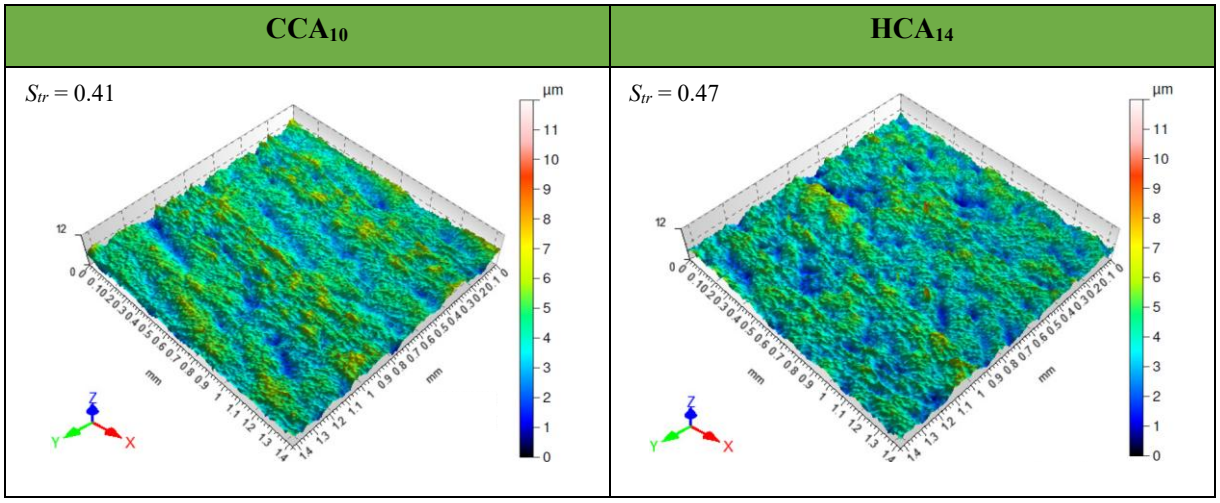
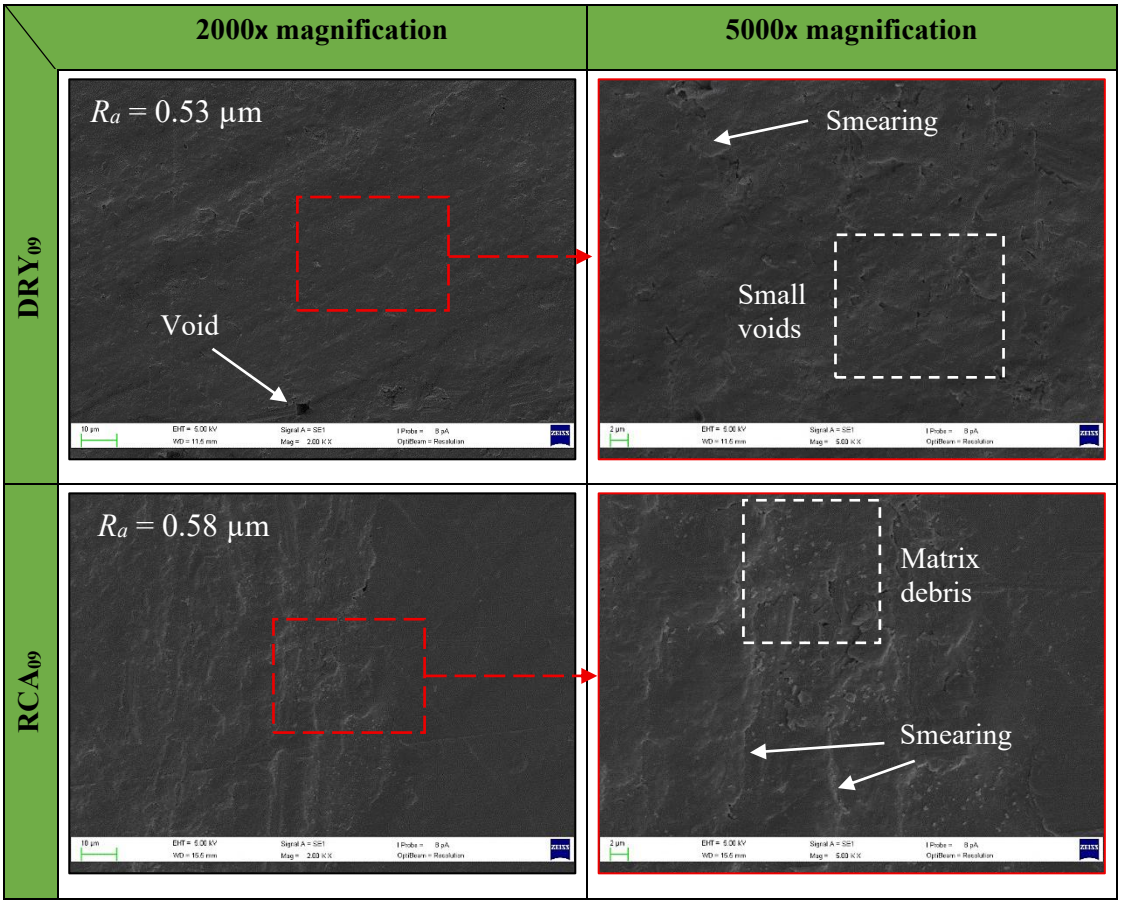


Fig. 6. 3D morphology of the samples with lower R_a values for each thermal condition

Fig. 7 presents the SEM images of the machined surfaces obtained under the different thermal conditions.



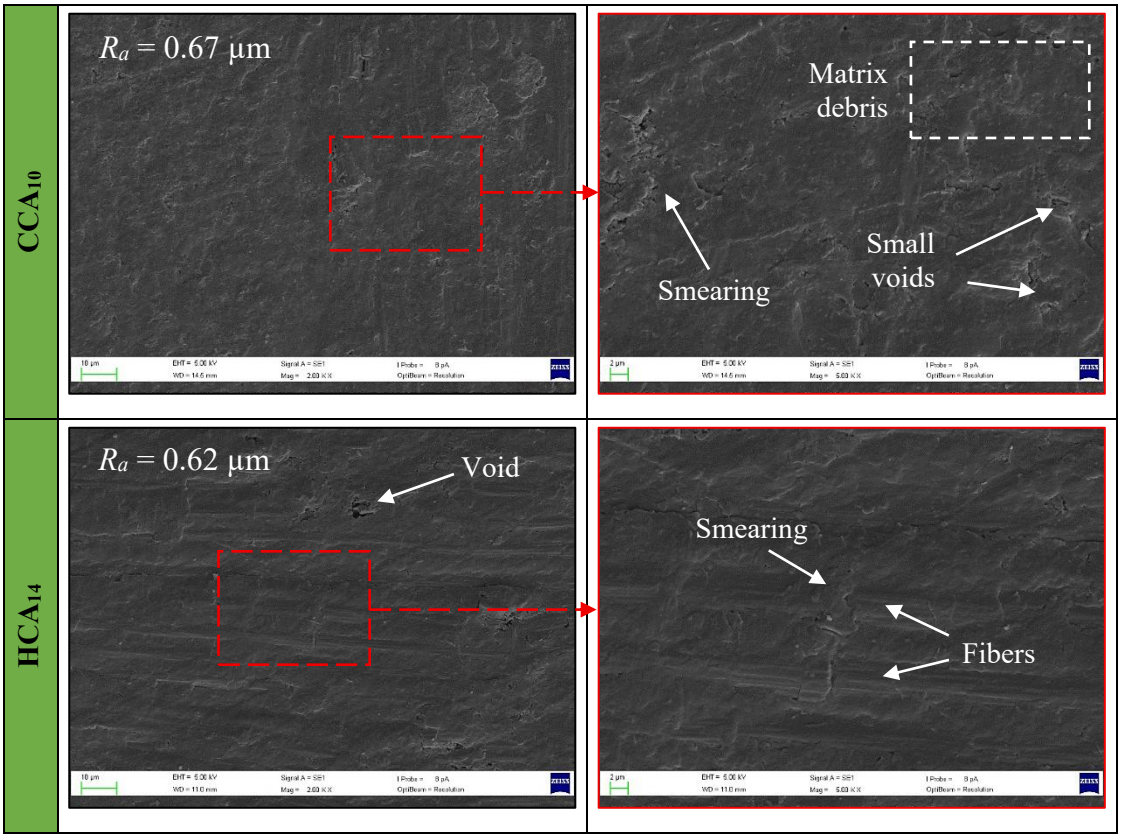


Fig. 7. SEM images of the samples with lower R_a values for each thermal condition

Under the DRY$_{09}$ condition, the surface exhibited good quality, with a low incidence of defects, characterized by small voids and low-intensity smearing, in agreement with the low roughness values obtained. Overall, all conditions resulted in surfaces with $R_a < 0.8$ µm, demonstrating the high efficiency of the insert in machining the material. Under the RCA$_{09}$ condition, the surface exhibited fewer imperfections than the CCA condition, with only matrix debris and low-intensity smearing, and no void formation, indicating greater surface uniformity. Under the CCA$_{10}$ condition, the surface appeared relatively uniform at 2000×, with no evident defects, whereas at 5000×, smearing, matrix debris, and small voids were identified. This behavior may be associated with the rapid cooling promoted by cooled air, which favors the solidification of plastically deformed material and the adhesion of matrix debris to the machined surface [27]. Finally, under the HCA$_{14}$ condition, a satisfactory surface texture was observed, with a low occurrence of matrix debris, possibly due to the heated airflow, which promotes the removal of debris before it adheres to the surface. Discrete regions of fiber exposure and slight smearing were also observed.

Overall, the results demonstrate that surface roughness during face milling of the CW50/PEEK composite using a PCD tool is strongly influenced by the thermal conditions, although to a lesser extent than might be expected due to the superior properties of the tool. The surface texture analyses indicate that thermal conditions that promote controlled matrix softening, such as HCA and, to a lesser extent, DRY, tend to provide better surface finish, whereas more intensive cooling (CCA) may increase the occurrence of defects associated with brittle fracture and the adhesion of matrix fragments. Furthermore, the limited statistical significance of the cutting conditions under some conditions reinforces the predominant role of thermal effects and tool characteristics in determining surface integrity. From a practical perspective, DRY stands out as the most feasible alternative, combining low operating costs with excellent performance in terms of machining force and surface roughness, as well as a low incidence of surface defects. Therefore, it is highly recommended for machining the composite investigated in this study.

4. CONCLUSIONS

This study evaluated the influence of different thermal conditions (DRY, RCA, CCA, and HCA) on the face milling of CW50/PEEK composite using a PCD tool, with a focus on machining force (F_U) and surface texture. The main findings are summarized as follows:

- The DRY and HCA conditions provided the lowest mean F_U values (14.5 N and 21.2 N, respectively), possibly due to thermal softening of the matrix. In contrast, the CCA and RCA conditions resulted in higher mean F_U values (30.8 N and 29.9 N, respectively) due to heat removal, which likely increased the resistance of the matrix to deformation. The standard deviations of F_U were approximately the same under the DRY, RCA, and HCA conditions (≈4.1 N), whereas the largest variation was observed under CCA (≈9.6 N), suggesting that the effect of intensified cooling on F_U is associated with variations in the cutting conditions.
- The ANOVA of F_U demonstrated that the reduction in temperature associated with the application of CCA and RCA decreased the process sensitivity to the cutting conditions. Conversely, the increase in temperature under the DRY and HCA conditions resulted in better statistical model fits.
- All thermal conditions produced arithmetic mean surface roughness (R_a) values below 1.0 μm. The DRY_{09} sample exhibited the lowest R_a value (0.53 μm), followed by RCA_{09} (0.58 μm),

HCA_{14} (0.62 µm), and CCA_{10} (0.67 µm). In addition, the RCA and HCA conditions exhibited the lowest variability in the results (0.68 ± 0.10 µm and 0.71 ± 0.09 µm, respectively), with both conditions falling within ISO roughness grade N6.

- The ANOVA of *Ra* under the CCA and HCA conditions indicated a limited influence of the cutting conditions and a predominance of thermal effects. In contrast, under the DRY and RCA conditions, the quadratic effect of axial depth of cut ($a_p \times a_p$) was statistically significant, while under the DRY condition, the interaction between cutting speed and feed per tooth ($v_c \times f_z$) was also significant.
- The 3D topography confirmed the high surface quality of the four samples with the lowest R_a values. The 3D roughness parameters exhibited low variation (S_a = 0.48–0.53 µm, S_q = 0.60–0.67 µm, and S_z = 6.40–8.27 µm). Greater surface uniformity was observed for the CCA_{10} and HCA_{14} samples, which exhibited texture aspect ratio (*Str*) values closer to the transition threshold toward an isotropic surface (*Str* > 0.5).
- SEM images confirmed that the CCA_{10} sample exhibited the poorest surface finish, with a higher incidence of defects such as smearing, matrix debris, and voids, associated with the more brittle behavior of the matrix at low temperatures. The HCA_{14} and DRY_{09} samples exhibited better surface quality, with HCA_{14} showing particularly favorable behavior due to the negligible occurrence of matrix debris.

Overall, the thermal conditions played a dominant role in the face milling response of CW50/PEEK. From an industrial perspective, the DRY condition stands out due to its simplicity, low cost, and competitive performance, whereas HCA shows potential for applications requiring greater surface uniformity. Future studies should consider in situ temperature measurements and different tool–material combinations to further elucidate the interactions governing the machining behavior of CW50/PEEK.

5. ACKNOWLEDGEMENTS

The authors thank Ensinger® Co. for the donation of TECATEC PEEK MT CW50 workpiece, Sandvik Coromant Co. for the donation of PCD milling inserts, Minitab® 22 for the trail test license for statistical analysis, Multiuser Center for Materials Characterization (CMCM/UTFPR) for the 3D roughness analysis, Brazilian Federal Agency for Support and Evaluation of Graduate Education (CAPES) (Grant No. 88887.840963/2023-00) for a student scholarship.

6. FUNDING

This work was supported by the Coordenação de Aperfeiçoamento de Pessoal de Nível Superior (CAPES) [Grant No. 88887.840963/2023-00]. The Federal Institute of Santa Catarina (IFSC) provided institutional support through Process No. 23292.030882/2022-26.

7. CREDIT AUTHORSHIP CONTRIBUTION STATEMENT

- **Carlos A. G. Aita:** Conceptualization, Methodology, Investigation, Formal analysis, Data curation, Visualization, Writing – original draft, Writing – review & editing.
- **André J. Souza:** Conceptualization, Methodology, Supervision, Validation, Writing – review & editing.
- **Émerson S. Passari:** Methodology, Investigation, Validation, Writing – review & editing.

8. COMPETING INTERESTS: STATEMENTS AND DECLARATIONS

No potential conflict of interest was reported by the authors.

9. DECLARATION OF GENERATIVE AI AND AI-ASSISTED TECHNOLOGIES IN THE MANUSCRIPT PREPARATION PROCESS

During the preparation of this work, the authors used ChatGPT (OpenAI) to assist with textual orthographic and grammatical editing and to aid the organization and refinement of some parts of the manuscript. After using this tool, the authors take full responsibility for the content of the published paper.

10. ETHICAL STANDARDS

The manuscript does not contain clinical studies or patient data.

11. REFERENCES

1. Thiruchitrambalam M, Bubesh Kumar D, Shanmugam D, et al. A review on PEEK composites - Manufacturing methods, properties and applications. *Materials Today: Proceedings* 2020, 33: 1085–1092.

2. Zol SM, Alauddin MS, Said Z, et al. Description of Poly(aryl-ether-ketone) Materials (PAEKs), Polyetheretherketone (PEEK) and Polyetherketoneketone (PEKK) for Application as a Dental Material: A Materials Science Review. *Polymers* 2023; 15: 2170
3. Liu K, Zhang J, Li J, et al. Experiment study of surface formation mechanism during cryogenic turning of PEEK. *Journal of Manufacturing Process* 2023; 104: 322–333.
4. Qin X, Wu X, Li H, et al. Numerical and experimental investigation of orthogonal cutting of carbon fiber-reinforced polyetheretherketone (CF/PEEK). *The International Journal of Advanced Manufacturing Technology* 2022; 119: 1003–1017.
5. Mata F, Gaitonde VN, Karnik SR, et al. Influence of cutting conditions on machinability aspects of PEEK, PEEK CF 30 and PEEK GF 30 composites using PCD tools. *Juornal Materials Processes Technology* 2009; 209: 1980–1987.
6. Alarifi IM. A Review on Factors Affecting Machinability and Properties of Fiber-Reinforced Polymer Composites. *Journal of Natural Fibers* 2023; 20: 2154304.
7. Rajak DK, Pagar DD, Menezes PL, et al. Fiber-reinforced polymer composites: Manufacturing, properties, and applications. *Polymers 2019*; 11:1667.
8. Zhao W, Yu R, Dong W, et al. The influence of long carbon fiber and its orientation on the properties of three-dimensional needle-punched CF/PEEK composites. *Composite Science Technology* 2021; 203: 108565.
9. Cao H, Liu L, Wu B, et al. Process optimization of high-speed dry milling UD-CF/PEEK laminates using GA-BP neural network. *Composite B Engineering* 2021; 221: 109034.
10. Caggiano A. Machining of Fibre Reinforced Plastic Composite Materials. *Materials* 2018; 11: 442.
11. Ferreira BM, Basso I, AF Toti et al. Cryogenic drilling of carbon fibre reinforced thermoplastic and thermoset polymers. *Composite Structure 2020* ; 251: 112625.
12. Devitte C, Souza AJ, Amorim HJ. Impact of cooled compressed air and high-speed cutting on the drilling of hybrid composite-metal stacks. *The International Journal of Advanced Manufacturing Technology* 2023; 125: 5445–5461.
13. Cao H, Song Y, Wu B, et al. A force model of high-speed dry milling CF/PEEK considering fiber distribution characteristics. *Journal Manufacturing Process* 2021; 68: 602–615.
14. Yuan W, Yang T, Liu C, et al. Towards understanding the thermal characteristics of thermoplastic CF/PEEK composite drilling: heat transfer mechanism, crystallinity, and hole

making performance. *International Journal of Advanced Manufacturing Technology* 2024; 130: 1075–1092.

15. Astakhov VP. Ecological Machining: Near-dry Machining. *Machining*. London: Springer London, pp. 195–223.
16. Kouam J, Songmene V, Balazinski M. et al. Effects of minimum quantity lubricating (MQL) conditions on machining of 7075-T6 aluminum alloy. *The International Journal of Advanced Manufacturing Technology* 2015; 79: 1325–1334.
17. Cococcetta N, Jahan MP, Schoop J, et al. Post-processing of 3D printed thermoplastic CFRP composites using cryogenic machining. *Journal Manufacturing Process* 2021; 68: 332–346.
18. Yildiz Y, Sundaram MM. Cryogenic machining of composites. *Machining Technology for Composite Materials*. Elsevier, 2012, pp. 365–393.
19. Danish M, Gupta MK, Rubaiee S, et al. Machinability investigations on CFRP composites: a comparison between sustainable cooling conditions. *The International Journal of Advanced Manufacturing Technology* 2021; 114: 3201–3216.
20. Abish J, Samal P, Narenther MS, et al. Assessment of drilling-induced damage in CFRP under chilled air environment. *Materials and Manufacturing Processes* 2018; 33: 1361–1368.
21. Domingo R, de Agustina B, Marín MM. Study of drilling process by cooling compressed air in reinforced polyether-ether-ketone. *Materials* 2020; 13: 1965.
22. Klein RF, Hoffmann N, Souza AJ, et al. Optimization of Cutting Parameters for Finish end Milling CFRP Under Vortex-Cooled Compressed Air. *Materials Research* 2022; 24: 2.
23. Shokrani A, Dhokia V, Newman ST. Environmentally conscious machining of difficult-to-machine materials with regard to cutting fluids. *International Journal Machine Tools and Manufacturing* 2012; 57: 83–101.
24. Nor Khairusshima MK, Che Hassan CH, Jaharah AG, et al. Effect of chilled air on tool wear and workpiece quality during milling of carbon fibre-reinforced plastic. *Wear* 2013; 302: 1113–1123.
25. Jia Z, Fu R, Wang F, et al. Temperature effects in end milling carbon fiber reinforced polymer composites. *Polymers Composites* 2018; 39: 437–447.

26. Pasquali F, Aita CAG, Souza AJ, et al. Influence of cooled and heated compressed air on the surface finish in face milling of CF30-reinforced PEEK. *Journal of Thermoplastic Composite Materials* 2026; 39: 4329–4351.
27. Aita CAG, Souza AJ, Passari ÉS, et al. Effect of cooled compressed air on the machining force and surface roughness generated by face milling of CW50/PEEK. *International Journal of Machining and Machinability of Materials* 2025; 27: 345–368.
28. Victrex PLC. *Improving Cryogenic Performance with Victrex Ct™ Polymers*. Lancashire, 2020.
29. Garcia-Gonzalez D, Rodriguez-Millan M, Rusinek A, et al. Low temperature effect on impact energy absorption capability of PEEK composites. *Composite Structure* 2015; 134: 440–449.
30. Hou G, Luo B, Zhang K, et al. Investigation of high temperature effect on CFRP cutting mechanism based on a temperature controlled orthogonal cutting experiment. *Composite Struct*ure 2021; 268: 113967.
31. Kim DC, Kim DY, Kang YS, et al. Experimental investigation of heat-assisted CFRTP drilling with an industrial robot. *Journal of Manufacturing Process* 2024; 124: 68–79.
32. Song Y, Chen X, Liu J, et al. Size Effect-Driven Dynamic Cutting Force Prediction in High-Speed Dry Milling of Plain-Woven CF/PEEK. *Polymers Composites* 2026; 47: 2072–2087.
33. Song Y, Chen X, He J. Multiphase structure-driven specific cutting energy modeling of plain wove CF/PEEK HSD milling. *Journal of Manufacturing Process* 2025; 156: 313–325.
34. Ensinger. Technical Data Sheet: TECATECPEEK CW50 black. *Ensinger GmbH*.
35. ISO 21920-3. Geometrical product specifications (GPS) – Surface texture: Profile, Part 3: Specification operators. *International Organization for Standardization*.
36. Wang Q, Fu L, Wang M, et al. Investigation of Machining Characteristics and Parameter Optimization for Laser-Assisted Milling of CF/PEEK Composites. *Micromachines*; 16: 2.
37. Guo X, Chen T, Li C, et al. Mechanism and machining quality in gyroscopic milling of thermoplastic carbon fiber reinforced PEEK composites. *Composite B Engineering*; 314: 113478.
38. Yan X, Zhao H, Wen Z, et al. Investigation on grinding temperature characteristics of CF/PEEK and material removal mechanism under temperature treatments. *Composite Science Technology* 2024; 252: 110621.

39. Montgomery DC. *Design and analysis of experiments*. John Wiley & Sons, Inc., 2013.
40. Murthy BRN, Harisha SR, Divya Deepak G, et al. Experimental Design and Optimization of Machining-Induced Cutting Force and Its Effect on Surface Roughness during Milling of Fiber-Reinforced Polymer Composites. *Journal of Composites Science 2024*; 8: 9.
41. Meng Z, Liu S, Hu K, et al. A review on the cutting of carbon fiber reinforced thermoplastic composites. *Polymers Composites* 2024; 45: 13459–13479.
42. Li G, Rahim MZ, Pan W, et al. The manufacturing and the application of polycrystalline diamond tools – A comprehensive review. *Journal of Manufaturing Process* 2020; 56: 400–416.
43. Rodriguez I, Soriano D, Ortiz-de-Zarate G, et al. Effect of Tool Geometry and LCO2 Cooling on Cutting Forces and Delamination when Drilling CFRP Composites Using PCD Tools. *Procedia CIRP* 2022; 108: 752–757.
44. Pawlus P, Reizer R, Wieczorowski M. Functional Importance of Surface Texture Parameters. *Materials* 2021; 14: 5326.
45. Fedorov K, Fayazbakhsh K, Ravindran C. Surface roughness and dimensional tolerances in A319 alloy samples produced by rapid investment casting process based on fused filament fabrication. *The International Journal of Advanced Manufacturing Technology* 2022; 119: 4423–4437.